



Synthesis and spectral characterization of $\text{Co}_x\text{Mg}_{1-x}\text{Al}_2\text{O}_4$ as new nano-coloring agent of ceramic pigment

I.S. Ahmed*, S.A. Shama, M.M. Moustafa, H.A. Dessouki, A.A. Ali

Chemistry Department, Faculty of Science, Benha University, Benha City, Egypt

ARTICLE INFO

Article history:

Received 18 December 2008

Received in revised form 11 July 2009

Accepted 29 July 2009

Keywords:

Ceramic pigments

Diffuse reflectance spectroscopy (DRS)

Thermogravimetric analysis (TGA)

X-ray diffraction (XRD)

Particle size

Transmission electron microscopy (TEM)

ABSTRACT

New nano-blue ceramic pigments of $\text{Co}_x\text{Mg}_{1-x}\text{Al}_2\text{O}_4$ ($0 \leq x \leq 0.1$) have been prepared by co-precipitate-combustion as a hybrid method using urea as a fuel at 500 °C in open furnace in air atmosphere. The structure of pigment is assigned based on TGA/DTA/DrTGA analyses, X-ray diffraction (XRD) and transmission electron microscopy (TEM). Also, electronic spectra, infrared (IR) and diffuse reflectance spectroscopy (DRS) using CIE $L^*a^*b^*$ parameter measurement techniques were used. The results revealed that the nano-particle size of pigments were obtained in the range 30–38 nm as well as the varying colors and particle size as a result of different calcinations temperatures within the range of 500–1200 °C for 2 h.

© 2009 Elsevier B.V. All rights reserved.

1. Introduction

The ceramic pigments based on traditionally doping of transition metal ions to matrix are the main subject for the preparation of pigments [1–7]. The doping cations associated with defects in crystal structure lead to the modification of physical properties of solid solution as a color [8–13]. The traditional source of blue color in ceramic pigment depended on cobalt ion [14]. Inorganic natural and synthetic pigments produced and marketed as fine powders are an integral part of many decorative and coatings and are used for the mass coloration of many materials, including glazes ceramic bodies and porcelain enamels [15,16]. The powders used for coloring ceramics must show thermal and chemical stability at high temperature and must be inert to the action of molten glass (frits or sintering aids) and also, the color of cobalt pigment depends on the coordination of Co^{2+} ions (tetrahedral coordination is preferred to octahedral) [17–19]. Ceramic pigments can be synthesized at low temperature by several solution techniques such as sol-gel [20], emulsion precipitation [21], hydrothermal [22], alkoxides hydrolysis [23], Penchini and co-precipitation method [24,25], low combustion method [26–29]. The advantages of the two latter methods synthesized crystalline powder with nanosize and high purity at low temperature. The synthesis routes are very important for determining the final properties of inorganic pigment as color, particle size, chemical and thermal stability. In this inves-

igation, the producing nano-crystalline of $\text{Co}_x\text{Mg}_{1-x}\text{Al}_2\text{O}_4$ spinel pigment using urea as a fuel and characterization by using different techniques.

2. Experimental

2.1. Materials and reagents

In particular, the starting chemicals used in this study were aluminum chloride hexahydrate ($\text{AlCl}_3 \cdot 6\text{H}_2\text{O}$), magnesium chloride hexahydrate ($\text{MgCl}_2 \cdot 6\text{H}_2\text{O}$), cobalt chloride hexahydrate ($\text{CoCl}_2 \cdot 6\text{H}_2\text{O}$) (Aldrich), sodium carbonate (Na_2CO_3) (Alfa), nitric acid 65% (Merck) and urea ($\text{CO}(\text{NH}_2)_2$) (Merck).

2.2. Synthesis of $\text{Co}_x\text{Mg}_{1-x}\text{Al}_2\text{O}_4$ ceramic pigment

The $\text{Co}_x\text{Mg}_{1-x}\text{Al}_2\text{O}_4$ pigments ($0 \leq x \leq 0.1$) were prepared by using metal salts of $\text{AlCl}_3 \cdot 6\text{H}_2\text{O}$, $\text{MgCl}_2 \cdot 6\text{H}_2\text{O}$ and $\text{CoCl}_2 \cdot 6\text{H}_2\text{O}$, and then dissolved in bid-stilled water, precipitated with sodium carbonate, good washing and drying. The above mixture was dissolved in nitric acid, heated to become clear solution, cooled to room temperature, and then urea was added as a complexion agent. The resulting solution was heated to ca. 80 °C for about 4 h until clear gel solution appears, transferred into furnace that was preheated to 500 °C. The precipitate initially started to swell and filled the beaker, producing a foamy precursor, this foam consists of very light and homogeneous flakes of very small particle size. The combustion reaction was completed within a few minutes and the ash voluminous and fluffy in nature of colored

* Corresponding author. Tel.: +20 (02) 0122408034/0133240199.
E-mail address: isahmed61@gmail.com (I.S. Ahmed).

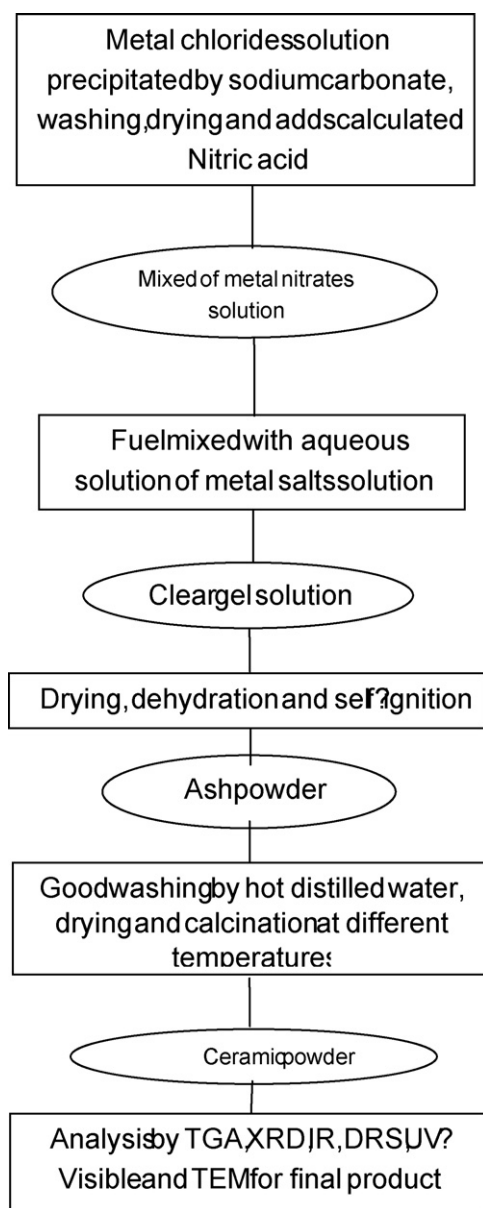


Fig. 1. The flow chart of preparation pigment powder and analysis methods.

powder was obtained. The flow chart of the process is shown in Fig. 1.

2.3. Instruments

Thermogravimetric analysis (TGA; TA Instruments, SDT2960) of the precursor was carried out at a heating rate of 10 °C/min in static air and in nitrogen atmosphere. Phase formation of product was identified by using X-ray diffraction (XRD; SIEMENS D5000) with Cu K α radiation. Transmission electron microscopy (TEM, modal EM 10 Zeiss, at 60 kV) was used to study the morphology of the synthesized powders by dispersing in water on a copper grid. The functional groups characterized by infrared (IR) spectroscopy in 400–4000 cm⁻¹ range for the calcinations powders at different temperature by using Jasco FT/IR-460 plus by employing potassium bromide KBr, pellet technique. The electronic spectra of ceramic pigments were measured by applying Nujol mull technique using Jasco 530 spectrophotometer with 10 mm matched Quartz cell. The diffuse reflectance of fired pigments was measured in Jasco spectrophotometer UV–vis in 300–800 nm range using standard

D65 illumination and barium sulfate as reference. The CIE- $L^*a^*b^*$ colorimetric method, recommended by the Commission Internationale de l'Eclairage (CIE) [30] was followed. In this method, L^* is lightness axis: black (0)–white (100), b^* is the blue (–)–yellow (+), a^* is the green (–)–red (+) axis and $\Delta E^2 = (L^*)^2 + (a^*)^2 + (b^*)^2$.

3. Results and discussion

3.1. The effect of fuel

A good fuel used in a combustion process should react non-violently, produce non-toxic gases, and act as a complex agent for metal cations [31]. The complexes were precipitated with increasing the ionic product of metal cations, thereby preventing preferential crystallization as the water in the precursor solution evaporates and the solution becomes gelatinous. For different metal cations, organic fuel with different ligand groups, i.e. carbonyl group and/or amine group (urea) may exhibit different complex power compared with 3-methyl-pyrozole-5-one (3MP5O) [32], which is one of the important factors that affect the phase formation and morphology of the final product. In addition, the chemical energy released from the exothermic reaction between various metal nitrates and fuel is different. This is another important factor that affects the phase formation of the final product because high temperature is in favor of the stable phase formation and particle aggregation of the final product.

3.2. Thermal analysis

The thermal analysis was performed of urea system. From TG-curves (Fig. 2), the weight losses were calculated for the dif-

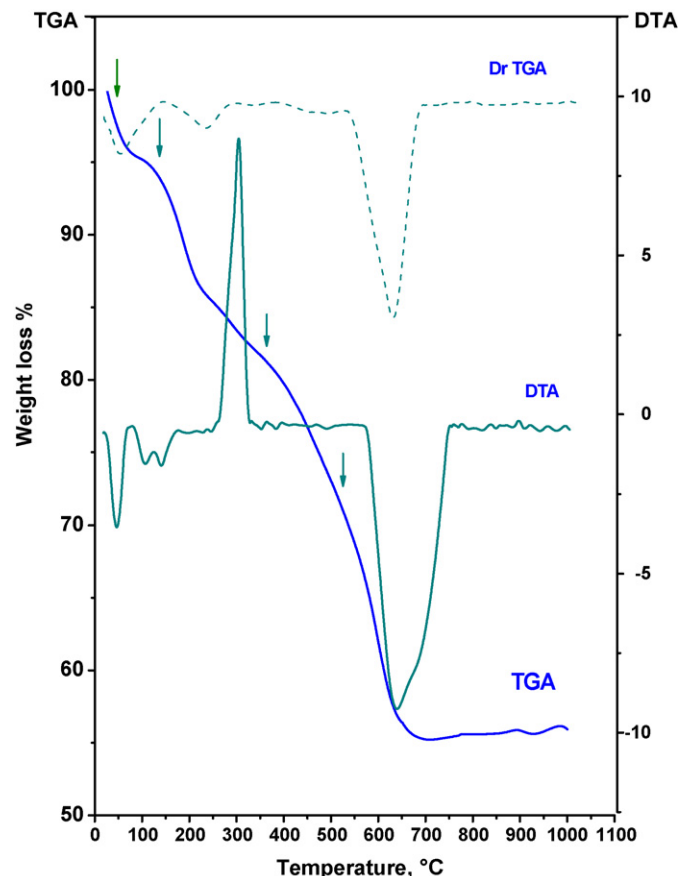


Fig. 2. Thermal analysis for 0.05 mol of Co²⁺ using urea as fuel.

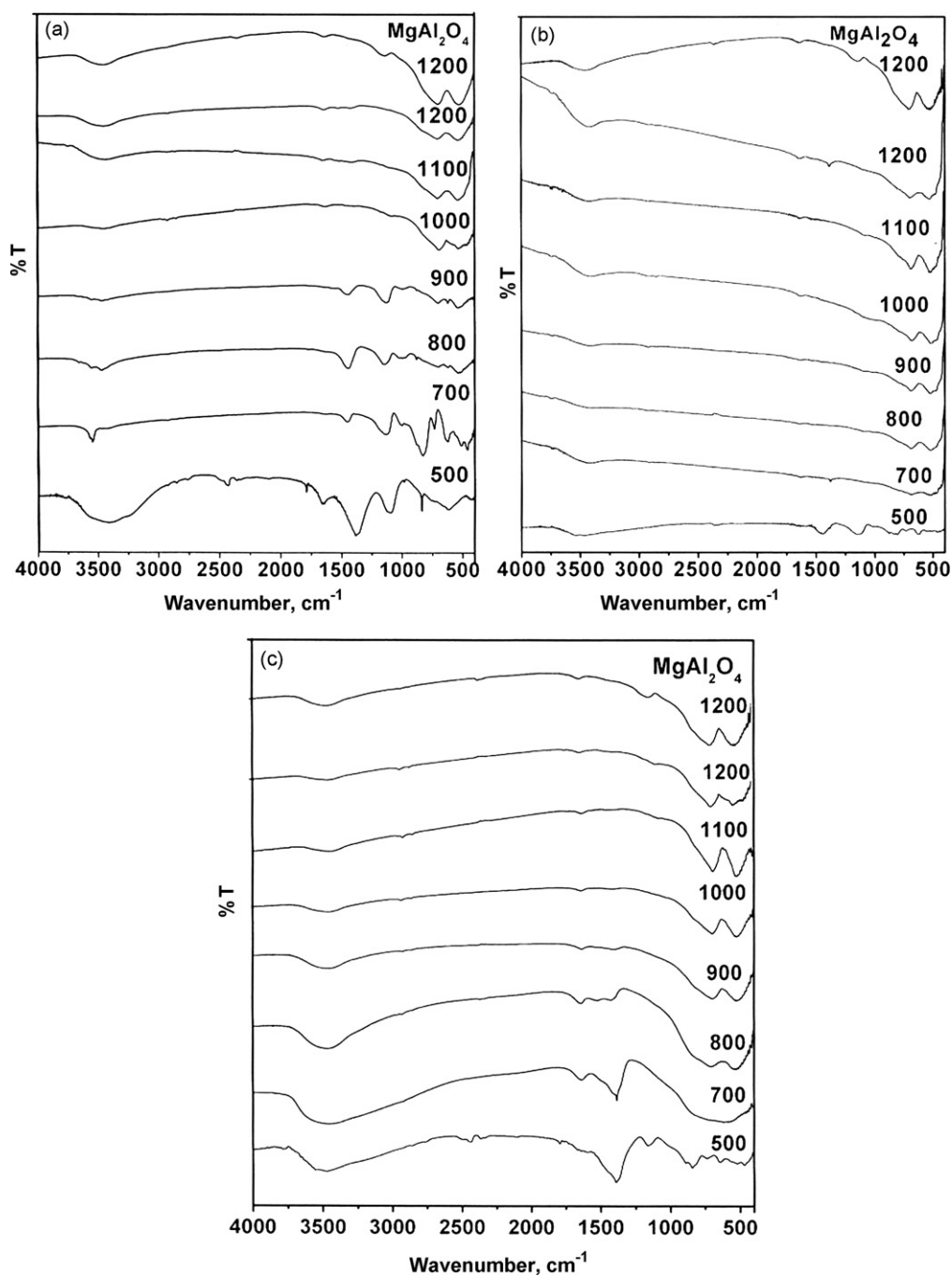


Fig. 3. Infrared spectra for 0.01 mol (a), 0.05 mol (b) and 0.10 mol (c) of Co^{2+} using urea as a fuel at different calcinations temperatures.

ferent steps. The first and second weight losses are 8.5, 11.7 and 15.6% and 10, 18 and 25.4% at temperature up to 250 °C and are attributed to the loss of hydrated and coordinated water molecules with endothermic peaks for urea systems, respectively. Whereas, the third and fourth weight loss are 18, 20.1 and 22% and 20, 22.5 and 23.58% within the 250–550 °C temperature range which are assignable to the evolution of NO_x , CO, and CO_2 gases with exothermic peaks. The $\text{Co}_x\text{Mg}_{1-x}\text{Al}_2\text{O}_4$ blue pigments were prepared by the thermal decomposition of the urea complexes and solution combustion of redox mixture. The fuel rich redox compounds ignite $\approx 400^\circ\text{C}$ and combust in air autocatalytically to yield voluminous, fine particles and large surface area blue pigments.

3.3. Infrared spectra

Infrared spectra for 0.01, 0.05 and 0.1 mol of Co^{2+} by using urea as a fuel are shown in Fig. 3. The result revealed that the broad band observed at 3450 cm^{-1} related to the stretching vibration of free ($-\text{OH}$) group of water molecule. The bands at 1778 and 1100 cm^{-1} are attributed to the stretching vibration of carbonyl, $\nu_{(\text{C}=\text{O})}$, $\nu_{(\text{C}-\text{O})}$ groups of residual organic fuel and the absorption bands at 1658, 1383 and 825 cm^{-1} correspond to undecomposed nitrate ions. Weak bands observed in the region $400\text{--}700\text{ cm}^{-1}$ for formation trace amounts of metal oxide. After calcinations at different temperatures from 500 to 1200°C , the observed bands in the region $800\text{--}4000\text{ cm}^{-1}$ are decreased gradually until completely disap-

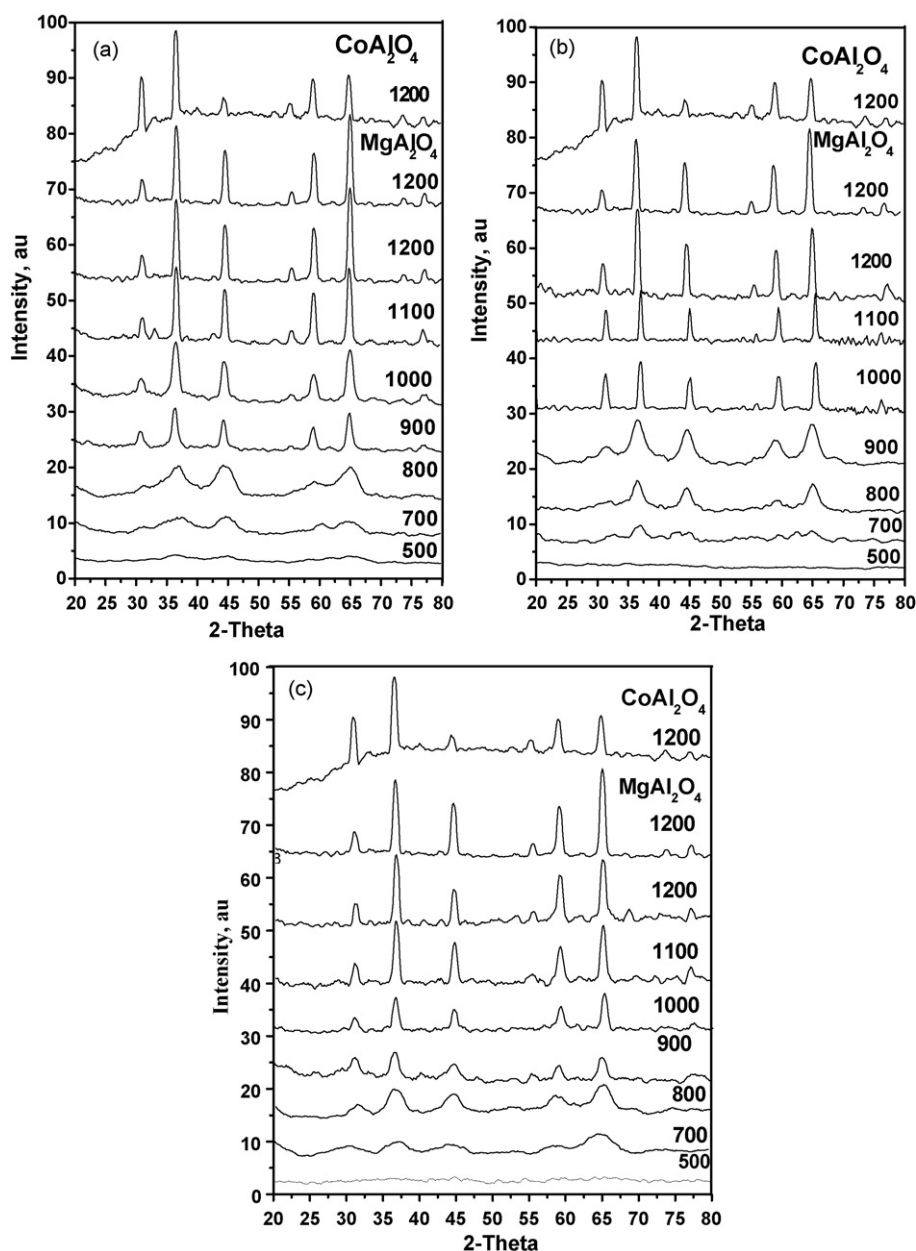


Fig. 4. X-ray diffraction for 0.01 mol (a), 0.05 mol (b) and 0.10 mol (c) of Co²⁺ at different calcinations temperatures using urea as a fuel.

peared at 1100 °C except, the strong vibration band at 3450 cm⁻¹ related to the stretching vibration of constitutional –OH group [33]. The appearance of strong bands lower than 800 cm⁻¹ corresponds to metal oxide. The two bands at 688 and 531 cm⁻¹ corresponding to AlO₆ groups are building up the magnesium spinel and two other bands at 520 and 450 cm⁻¹ corresponding to AlO₄ groups [34].

3.4. The X-ray diffraction and particle size measurements

The powder X-ray patterns of Co_xMg_{1-x}Al₂O₄ pigments show characteristic XRD reflections of spinel solid solution of CoAl₂O₄ and MgAl₂O₄. Fig. 4 shows that the results for X-ray powders calcined at different firing temperatures in range 500–800 °C observed in amorphous state and small crystallites that indicated in broadening lines. While, at 900 °C the calcinated powders begin to appear of the spinel crystalline form isomorphism phase. With increasing temperature above 900 °C, the intensities of peaks increase

gradually until sharpen peaks are observed 1200 °C. Table 1 shows the crystalline spinel phase content and the particle size increase with increasing calcinations temperatures. Fig. 5 shows the relation between the particle size calculated for 0.01, 0.05 and 0.10 mol of cobalt ion at different calcinations temperatures using urea as a fuel. From XRD at different calcinations temperatures it is revealed

Table 1

The particle size for 0.01 mol (a), 0.05 mol (b) and 0.1 mol (c) of Co²⁺ at different calcination temperatures using urea as a fuel.

System (mole of Co ²⁺)	Temperature, °C						
	500	700	800	900	1000	1100	1200
0.01	Am	3.38	4.54	18.7	21.1	34.89	46.33
0.05	Am	3	3.62	16.19	17.76	34.42	45.1
0.10	Am	4.22	8.58	15.78	19.72	32.21	43.58

Am: amorphous.

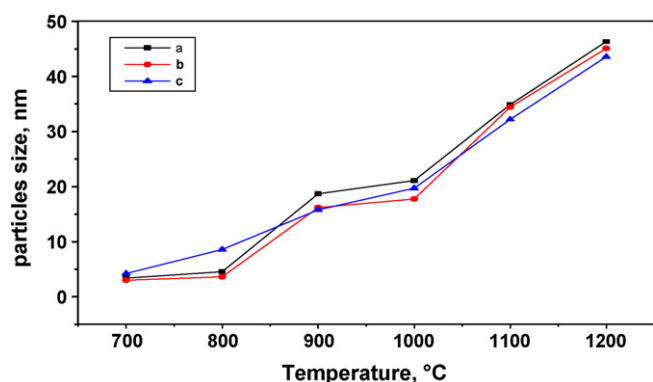


Fig. 5. The relation between particle size for 0.01 mol (a), 0.05 mol (b) and 0.1 mol (c) of Co^{2+} at different calcination temperatures using urea as a fuel.

that the calcinations temperatures effects on the particle size with increase of sintering temperature. The increasing of cobalt affected decrease of particle size of pigments, in range 46.33–43.58 nm at 1200 °C. The TEM photographs of samples show the sheet shape for 0.01 mol of cobalt and spherical particles for 0.05 and 0.1 mol of cobalt ion as doping as shown in Fig. 6. The particle size observed by XRD is in good agreement with that obtained from TEM as present in Table 2.

3.5. The diffuse reflectance spectroscopy (DRS) and electronic spectra

Diffuse reflectance spectroscopy (DRS) indicates the appearance of band around 510 nm at 700 °C that tends to pale blue color of

Table 2
XRD crystallite and TEM particle size different doping types at 1100 °C using urea as a fuel.

System (mole of Co^{2+})	Particle size, nm	
	X-ray	TEM
0.01	34.89	35
0.05	33.9	34
0.10	32.21	33.3

Table 3
Colorimetric data for different doping of 0.01, 0.05 and 0.1 mol of Co^{2+} at different calcinations temperatures using urea as fuel.

System (mole of Co^{2+})	Temperature, °C	L^*	a^*	b^*	ΔE
0.01	500	93.58	-1.55	0.90	94.10
	700	97.09	-0.96	-0.53	97.10
	800	96.64	-1.40	-1.09	96.60
	900	95.77	-1.01	-1.48	95.80
	1000	94.50	-0.91	-2.33	94.50
	1100	94.00	-0.67	-2.89	94.10
	1200	93.04	-0.85	-3.96	93.00
0.05	500	92.70	-1.05	0.08	92.71
	700	95.19	-1.70	-1.07	95.21
	800	95.00	-0.54	-2.38	95.03
	900	94.69	-0.76	-3.19	94.75
	1000	93.65	-0.58	-3.84	93.73
	1100	92.29	-0.76	-4.06	92.38
	1200	91.77	-0.72	-5.62	92.00
0.10	500	91.11	-1.61	0.73	91.13
	700	93.06	-1.38	-2.06	93.01
	800	92.39	-1.26	-3.71	92.47
	900	92.24	-0.96	-4.29	92.34
	1000	91.87	-1.11	-5.38	92.00
	1100	91.26	-1.00	-6.42	91.50
	1200	90.29	-0.74	-8.12	90.64

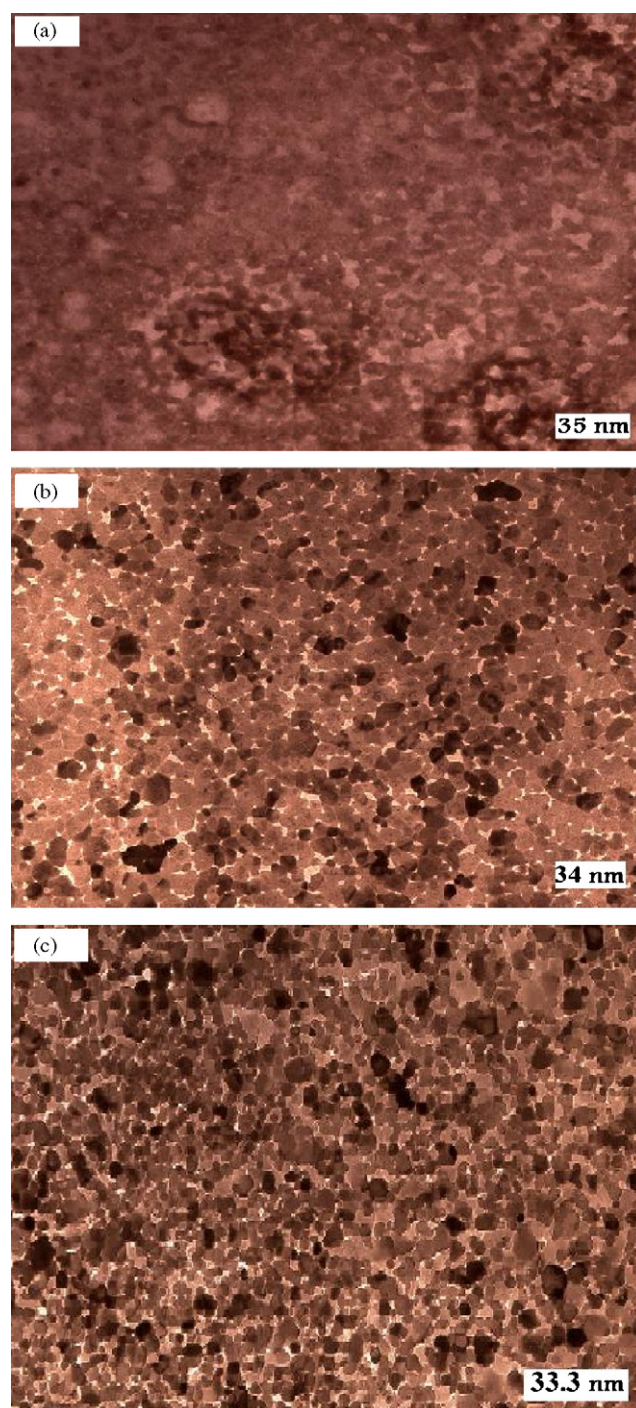


Fig. 6. TEM for 0.01 mol (a), 0.05 mol (b) and 0.10 mol (c) of Co^{2+} at 1100 °C using urea as fuel.

sample and this band shift to lower wavelength as calcinations temperatures increase until reaching around 500 nm at 1000 °C for blue color and 490 nm at 1200 °C [35–36]. Also, the results revealed that the values of a^* are random while L^* values decreases and b^* values increases in negative direction as a result of increasing calcinations temperatures, which is shown in Table 3 and Fig. 7. The defects in crystal structure lead to the distorted tetrahedral and octahedral sites in spinel structure, changing the ligand-field around the chromophore and hence changing the observed color [37]. The increase in negative values of b^* , the higher intensity of blue color, and the decrease in L^* parameter tend to reduce the lightness of sample. In the same time, the increasing of amount cobalt percent, the value

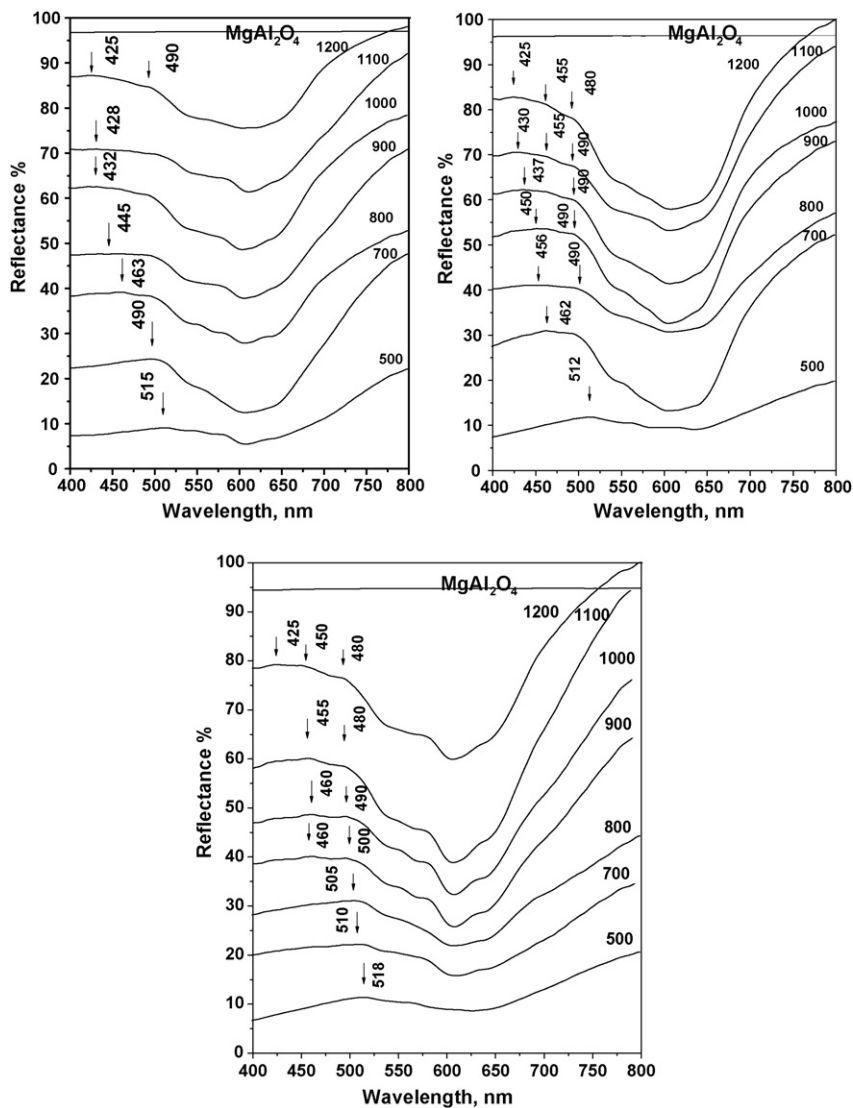


Fig. 7. Diffuse reflectance spectra for 0.01 mol (a), 0.05 mol (b) and 0.1 mol (c) of Co^{2+} at different calcination temperatures using urea as a fuel.

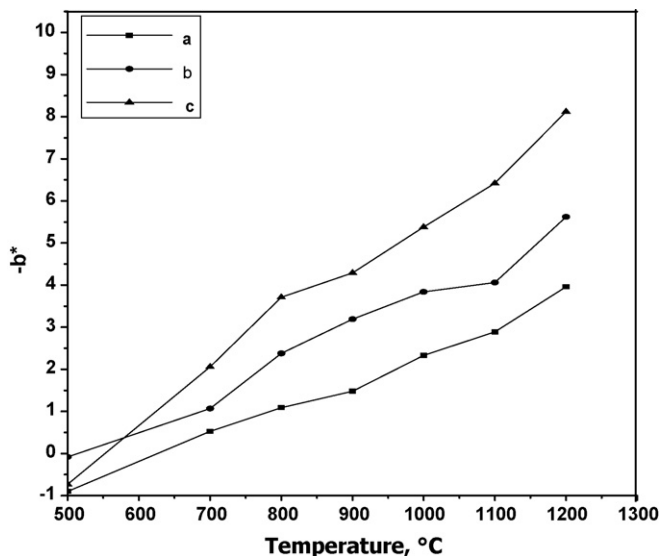


Fig. 8. Colorimetric data for 0.01 mol (a), 0.05 mol (b) and 0.1 mol (c) of Co^{2+} at different calcination temperatures using urea as a fuel.

of b^* increases as present in Fig. 8, leading to the depth of blue color as result of calcinations temperatures. The lower value of hue variation ΔE tends to a good color matching [38]. Colorimetric data show the high value of b^* and lower value of hue variation ΔE at 1200°C for all doping cobalt percents. This means that the appearance of good pigment powder color and a good color matching occurred at 1200°C . The color of different doping is shown in Fig. 9.

The electronic spectra of 0.01, 0.05 and 0.1 mol of cobalt ion as doping at different calcinations temperatures show that three broad absorption bands at 544 (green region), 580 (yellow–orange region) and 630 (red region) nm this indicates the tetrahedral coordination of cobalt [39]. Fig. 10 shows that the electronic spectra of 0.01 mol of cobalt ion at different calcinations temperatures using urea as fuel. The energy level diagram gives d–d transitions of cobalt



Fig. 9. Color for 0.01 mol (a), 0.05 mol (b) and 0.1 mol (c) of Co^{2+} at 1200°C using urea as a fuel.

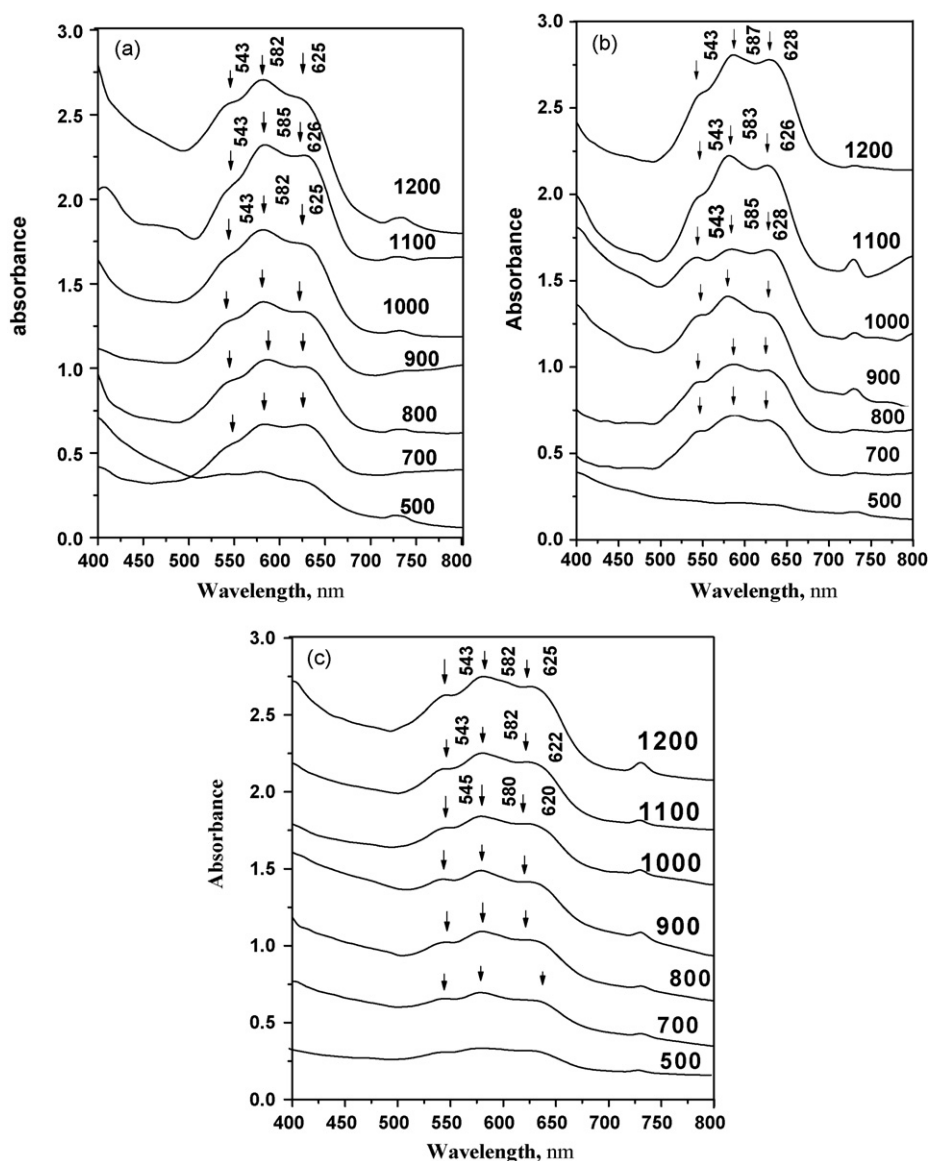


Fig. 10. The electronic spectra for 0.01 mol (a), 0.05 mol (b) and 0.10 mol (c) of Co^{2+} at different calcination temperatures using urea as fuel.

($3d^7$) from Orgel diagram, which shows the presence of three transition ${}^4A_2(F) \rightarrow {}^4T_2(F)$, ${}^4A_2(F) \rightarrow {}^4T_1(F)$ and ${}^4A_2(F) \rightarrow {}^4T_1(P)$. The wide and intense absorption band between 500 and 700 nm could be attributed to third transition from ${}^4A_2(F)$ ($e^4t^3_2$) as ground state to the excited ${}^4T_1(P)$ ($e^3t^4_2$) state. This triple band in visible region can be attributed to John-Teller distortion of tetrahedral structure according to Bamford [40], or to an interaction between L and S quantum numbers according to Bates [41].

4. Conclusion

The preparation of fine particle $\text{Co}_x\text{Mg}_{1-x}\text{Al}_2\text{O}_4$ as a coloring agent of blue ceramic pigments by the thermal decomposition of precursors gives nanosize oxides with particle sizes in the range of 3–18.7 nm using urea fuel at calcinations temperatures in range 700–900 °C. Whereas the increasing temperature yield pigments with particle size in the range 18.7–48 nm. The solid solution from two mixed phases CoAl_2O_4 and MgAl_2O_4 spinel were obtained with no phase separation and observed on sintering the solid solutions with higher Co^{2+} substitution in MgAl_2O_4 indicating the novelty of the combustion process. The powders were calcinated at different

temperatures and characterized by different tools as thermal analyses (TG/DTG/DTA), X-ray diffractions, UV–vis spectroscopy, diffuse reflectance spectra (CIE $L^*a^*b^*$ parameters) measurements, infrared spectroscopy (IR) and transmission electron microscopy (TEM).

References

- [1] S. Ekambaram, J. Alloys Compd. 390 (2005) 14–16.
- [2] K.C. Patil, S. Ghosh, S.T. Aruna, S. Ekambaram, The Indian Potter 1 (1996) 34.
- [3] K.C. Patil, S.T. Aruna, S. Ekambaram, Curr. Opin. Solid State Mater. Sci. 2 (1997) 156–165.
- [4] F. Fernandez, C. Colon, A. Duran, R. Barajas, A. d'Ors, M. Becerril, J. Llopis, S.E. Paje, R. Saez-Puche, I. Julian, J. Alloys Compd. 277 (1998) 750–753.
- [5] R.A. Eppler, Uhlmann's Encyclopedia Sci. Technol., A5, 1986, p. 545.
- [6] P. Maestr, E.P. Patent No. 0203838, 1985.
- [7] P. Macaudier, E.P. Patent No. 680930, 1995.
- [8] K. Sone, Y. Fukuda, Inorganic Thermochemistry, Springer-Verlag, Berlin, 1987.
- [9] S. Nakada, M. Yamada, T. Ito, M. Fujimoto, Chem. Lett. 1 (1977) 243.
- [10] D.R. Bloomquist, R.D. Willett, Thermochromic phase transitions in transition metal salts, Coord. Chem. Rev. 47 (1982) 125–164.
- [11] J.D. Lee, A New Concise Inorganic Chemistry, 3rd ed., ELBS, 1977.
- [12] Z. Halmos, W.W. Wendlandt, Electrical conductivity—differential thermal analysis measurements on some M_nHg_l complexes, Thermochim. Acta 7 (1973) 113–122.
- [13] M. Kurzawa, E. Tomaszewicz, Spectrochim. Acta A 55 (1999) 2889–2892.

- [14] R.K. Mason, *J. Am. Ceram. Soc. Bull.* 40 (1999) 2889.
- [15] G. Buxbaum, *Industrial Inorganic Pigments*, 2nd ed., Wiley-Vch, 1997.
- [16] M. Jansen, H.P. Letschert, *Nature* 404 (2000) 980.
- [17] G. Monari, T. Manfredini, *J. Ceram. Eng. Sci. Process.* 17 (1996) 102.
- [18] S. Meseguer, M.A. Tena, C. Gargori, J.A. Badenes, M. Llusar, G. Monrós, *Ceram. Int.* 33 (2007) 843–849.
- [19] D. Segal, Chemical synthesis of ceramic materials, *J. Mater. Chem.* 7 (1997) 1297–1305.
- [20] M. Jode, H. Mays, J. Schmidt, R. Willumeit, R. Schomacker, *Colloids Surf. A: Physchem.* 163 (2000) 3–15.
- [21] R.E. Riman, W.L. Suchanek, M.M. Lencka, *Ann. Chim. Sci. Mater.* 27 (2002) 15–36.
- [22] N.P. Castaing, F. Duboudin, J. Ravez, P. Hagenmuller, *Mater. Bull.* 22 (1987) 261.
- [23] M. Kakihana, *J. Sol-Gel Sci. Technol.* 6 (1996) 7.
- [24] R.A. Candeia, M.I.B. Bernardi, E. Longo, I.M.G. Santos, A.G. Souza, *Mater. Lett.* 58 (2004) 569–572.
- [25] R. Olazcuaga, G. Le Pollo, A. El Kira, G. Le Fleem, P. Maestro, *J. Solid State Chem.* 71 (1987) 57.
- [26] S.E. Tarling, G. Le polles, A. El Kira, G. Le Fleem, P. Maestro, *Acta Crystallogr. B* 44 (1988) 128.
- [27] J. Mahia, A. Viegro, J. Mira, M.A. Lopez-Quintela, S.B. Oserof, *J. Solid State Chem.* 122 (1996) 25.
- [28] M.D. Nersisyan, A.G. Peresada, A.G. Merzhanov, *Int. J. SHS* 7 (1998) 60.
- [29] Y. Li, J. Zhao, J. Han, X. He, *Mater. Res. Bull.* 40 (2005) 981–989.
- [30] CIE, Recommendations of Uniform Color Spaces, Color Difference Equations, Psychometrics Color Terms, Supplement No. 2 of CIE Publ. No. 15 (E1-1. 31) 1971, Bureau Central de la CIE, Paris, 1978.
- [31] V.C. Sousa, A.M. Segadaes, M.R. Morelli, R.H.G.A. Kimina, *Int. J. Inorg. Mater.* 1 (1999) 235–241.
- [32] I.S. Ahmed, H.A. Dessouki, A.A. Ali, Synthesis and characterization of new nano particles as blue ceramic pigment, *Spectrochim. Acta A* 71 (2008) 616–620.
- [33] M.F.M. Zawrah, A.A. El Kheshen, *Br. Ceram. Trans.* 101 (2002) 71–74.
- [34] K. Nakamoto, *Infrared and Raman Spectra of Inorganic and Coordination Compounds*, 4th ed., Wiley Press, New York, 1986, p. 231.
- [35] M. Llusar, A. Fores, J.A. Badenes, J. Calbo, M.A. Tena, G. Monros, *J. Eur. Ceram. Soc.* 21 (2001) 1121–1130.
- [36] D.M.A. Melo, J.D. Cunha, J.D.G. Fernandes, M.I. Bernardi, M.A.F. Melo, A.E. Martinelli, *Mater. Res. Bull.* 38 (2003) 1559–1564.
- [37] J.D. Cunha, D.M.A. Melo, A.E. Martinelli, M.A.F. Melo, I. Maia, S.D. Cunha, *Dyes Pigments* 65 (2005) 11–14.
- [38] F. Bondioli, T. Manfredini, M. Romagnoli, *J. Eur. Ceram. Soc.* 26 (2006) 311–316.
- [39] T. Mimani, S. Ghosh, *Curr. Sci.* 78 (2000) 892–896.
- [40] C.R. Bamford, *Phys. Chem. Glasses* 3 (1962) 189–202.
- [41] T. Bates, *Ligand field theory and absorption spectra of transition-metal ions in glasses Modern Aspects of the Vitreous State*, vol. 2, Butterworths, London, 1961, pp. 195–254.